

Random forest method for predicting discharge current waveform and mode of dielectric barrier discharges

Laiadi Abdelhamid¹, Chentouf Abdellah¹, Ezziyyani Mostafa²

¹Laboratory of applied physics, Physics Department, FSTT, UAE University, Tangier, Morocco

²Mathematics and Application Laboratory, FSTT, UAE University, Tangier, Morocco

Article Info

Article history:

Received May 25, 2024

Revised Jan 17, 2025

Accepted Mar 25, 2025

Keywords:

Cold atmospheric plasma

Dielectric barrier discharge

Filamentary mode

Homogeneous mode

Machine learning

Random forest

ABSTRACT

This study addresses the classification of Homogeneous and Filamentary discharge modes in dielectric barrier discharge (DBD) systems and predicts the Homogeneous current waveform using machine learning (ML). The motivation stems from the need for accurate modelling in non-thermal plasma systems. The problem tackled is distinguishing between these two modes and predicting the current waveform for Homogeneous discharge. A random forest classification algorithm is applied, using experimental features such as applied voltage, frequency, gas gap, dielectric material, and gas type. An exponential model is proposed for the discharge current, with Gaussian regression transforming the model's parameters. The classification results are evaluated through a confusion matrix, showcasing 80% accuracy in distinguishing discharge modes. The regression analysis reveals strong Pearson correlation coefficients between predicted and experimental waveforms. In conclusion, the results demonstrate the efficacy of ML techniques in enhancing DBD system modelling, though improvements can be made by expanding the dataset and refining feature selection for better classification and prediction performance.

This is an open access article under the [CC BY-SA](#) license.



Corresponding Author:

Laiadi Abdelhamid

Laboratory of applied physics, Physics Department, FSTT, UAE University

Tangier, Morocco

Email: hamidlaiadi@gmail.com

1. INTRODUCTION

Dielectric barrier discharge (DBDs), also known as silent discharges, are considered the simplest way to obtain non-thermal plasma (also known as cold-plasma) in the laboratory at atmospheric pressure. To prevent the formation of an electric arc, at least one dielectric barrier is used between cylindrical or two planar electrodes, which are connected to an alternative or pulsed power supply [1]. DBDs have numerous applications in the domains of industry [2], medicine [3], and environment [4].

DBDs have two modes, Homogeneous and Filamentary. The Homogenous discharge mode is typically produced when gases such as Helium, Neon, Argon are used [5]. Generally, the current waveform of Homogeneous discharge is characterized by a single pulse in each half cycle of the applied voltage, the homogenous discharge mode may manifest as Atmospheric pressure glow discharge (APGD) or Atmospheric pressure Townsend discharge (APTD) [6], several factors could influence the waveform of the Homogeneous discharge current in DBD configuration as shown in Figure 1, including the applied voltage [7], the frequency of the applied voltage [8], the gas type [9], the gas gap distance [10], and the dielectric material [11].

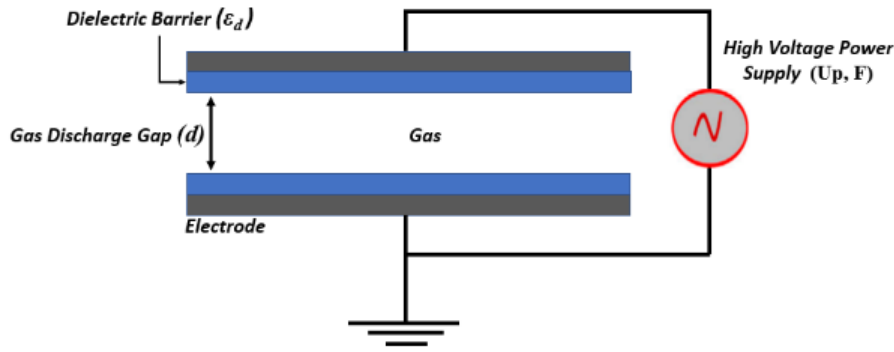


Figure 1. Dielectric barrier discharge configuration

In other hand the filamentary discharge mode is the most naturally occurred in DBD discharges, typically produced in Air, the waveform of the discharge current is characterized by random fluctuations describe the random distribution of micro-discharges in space and time [9]. In this work we aim to predict the discharge mode of DBD discharges using the selected experimental features, and to predict the discharge current waveform of the Homogeneous mode.

Given the abundant experimental data generated by cold plasma and DBD discharge systems, a recent paradigm in the field of cold plasma research involves the adoption of data-driven modelling [12]. For example ML methods have been employed to predict electrical characteristics of DBD systems [13], and simulate the low-temperature plasma [14]. Exploiting the diversity of current waveforms documented in the literature on Homogeneous and Filamentary DBD discharges, our study is driven by two main objectives. For the first objective, we aim to build a model to classify the discharge mode using the random forest classification algorithm, the second objective involves predicting the discharge current from the experimental features utilizing a ML algorithm, this latter objective unfolds in two steps: firstly, we aim to associate the experimental features for each current waveform with a set of defining of the proposed Gaussian model parameters by mediating the proposed exponential law of discharge. Secondly, the intention is to employ a random forest regression model to predict the relationship between each parameter of the discharge current model and the associated experimental features.

The outline of this paper is as follows: firstly, the data collection process and the selected features are described for both classification and regression tasks; secondly, the classifier model used to classify the discharge mode of the DBD discharge will be described, along with its results and evaluation. Subsequently, the proposed model for the discharge current will be suggested, and the extraction of parameters for regression will be introduced. Following this, the configuration and application of the random forest regression model are described, and the results derived from its application are evaluated.

2. METHOD

For the classification part the dataset was collected from 100 discharge experiments, and for the regression part, it was sourced from 33 Homogeneous DBD discharge experiments. Each discharge current waveform was sampled into 1,000 points with associated data including applied voltage amplitude, frequency of the applied voltage, gas gap, gas type, and dielectric material used. The gases employed in this work include: Air [8]-[11], [15], [16], Xenon [17], Helium [18], [19], Argon [6], Nitrogen [6], [20], and Neon [9], [21].

The geometric configurations of the dielectric barrier in the dataset are both planar and cylindrical. All experiments were conducted at atmospheric pressure. Table 1 illustrates a sampled example for the structure of the data collected, while Table 2 provides a statistical overview of the experimental feature values within the dataset.

Table 1. Structure of the classification data

Author	Voltage (kV)	Frequency (kHz)	Gap(mm)	Gas	Dielectric	Mode
Mangolini [19]	2	10	5	Helium	Alumina	Homogeneous
Garamoon [16]	5	0.05	1.1	Air	Quartz	Filamentary

Table 2. Statistic values of the features used in classification

	Voltage (kV)	Frequency (kHz)	Gap (mm)	Gas Breakdown(kV/mm)	Dielectric constant
Min	0.5	0.05	0.4	0.6	2.3
Max	25	150	10	22.5	11.54
Mean	6.76	14.94	2.61	9.83	6.4
Standard deviation	6.52	20	1.97	8.31	2.34

3. CLASSIFICATION MODEL

As some features in Table 1 are categorical, encoding becomes necessary. Specifically, the dielectric material was encoded into its corresponding dielectric constant, while the gas type was encoded based on its average breakdown voltage at atmospheric pressure. Moreover, the target value, representing the discharge mode, was encoded into a binary class (0 for Homogeneous and 1 for Filamentary), facilitating streamlined classification processes.

3.1. Random forest for classification

A machine learning approach [22], specifically the random forest classification algorithm [23] is adopted to predict and model the inherently non-linear relationship between the discharge mode and associated features of the discharge experiment. Random forest algorithm combines several decision trees as shown in Figure 2 to create a more accurate model by selecting random subsets of data and features, then aggregating the results to make a final prediction through majority voting.

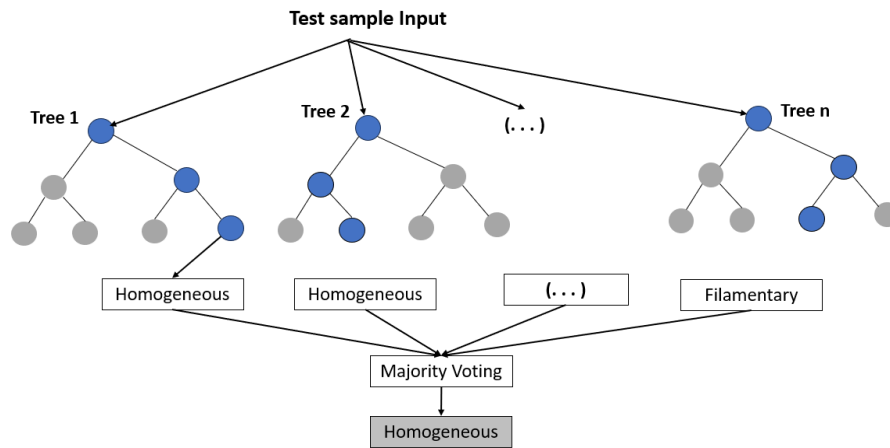


Figure 2. Random forest classification algorithm

The features chosen for classification can be encapsulated within a vector $X_c = [U_p, d, V_{bd}, \epsilon_d]$, where U_p denote the applied voltage amplitude, d the gas gap distance, V_{bd} the breakdown voltage of the gas, and ϵ_d denote the material dielectric constant. The target vector is denoted as $y_c = ['Homogeneous', 'Filamentary']$. For the random forest classifier (RFC) algorithm, the chosen hyperparameters include the number of trees ($n_{estimators} = 120$), and the criterion used is 'entropy'. The training data is used to train the classifier model by providing input features and corresponding target values. The test data, comprising 20% of the total dataset, is reserved to evaluate how well the trained RFC performs on new, unseen data.

3.2. Classification results and evaluation

3.2.1. Confusion matrix

A confusion matrix provides an overview of the classifier's performance by illustrating the predicted classes against the actual ones. In Figure 3, the confusion matrix for our classifier is presented, which offers a clear visualization of the random forest classification model's performance by comparing predicted classes against actual discharge modes. In this matrix, the rows represent the actual discharge modes (Homogeneous or Filamentary), while the columns represent the predicted modes.

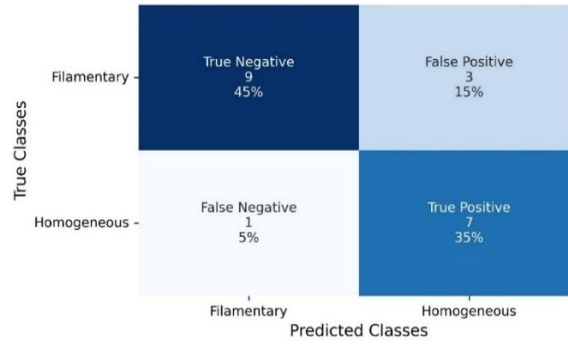


Figure 3. Confusion matrix of the classification model

3.2.2. Model evaluation and discussion

Accuracy in classification models is a metric that measures the proportion of correctly predicted instances among all instances in the dataset. It provides an overall assessment of the model's ability to correctly classify different classes or categories. Accuracy is calculated as follows:

$$Accuracy = \frac{T_p + T_n}{T_p + T_n + F_p + F_n}$$

where T_p , T_n , F_p , F_n denotes true positive, true negative, false positive, and false negative respectively, by analysing this confusion matrix, for example, the model has made 3 false positive predictions, i.e., it has predicted the presence of 3 discharges with Homogeneous modes, whereas in reality they are Filamentary, the accuracy of our classification model is 0.8.

Achieving 80% accuracy in our classification model is a positive result, but it is essential to explore the implications of the false positive predictions. The misclassification of Filamentary discharges as Homogeneous reveals limitations in the model's ability to clearly distinguish between the two modes. This suggests that the model's sensitivity to subtle differences between these discharge types needs improvement. Further refinement of the model, particularly in its handling of nuanced features, could significantly enhance its classification performance.

4. REGRESSION MODEL

4.1. Proposed discharge current model

The discharge current is considered as an internal electrical parameter of DBD, it lacks an explicit expression, and it is difficult to measure it directly, the models addressing this current fall into two main categories: physical models, which employ numerical simulations to deduce the current waveform [24] and electrical models [15]. The hypothesis of this work is grounded on the simple electrical model for DBD, as illustrated in Figure 4. In this model, C_d and C_g denote the dielectric barrier capacitance and gas gap capacitance, respectively, while R_p represents the plasma discharge impedance (Figure 4(a)) [25].

The proposed model operates under certain assumptions: Firstly, the plasma discharge current $I_{\text{plasma}}(t)$ is conceptualized as the exponential law as in equation (1) (Figure 4(b)). Secondly, we suppose that the discharge current and the gap voltage waveforms exhibits symmetry with respect to the half cycle of the alternative applied voltage. The model $I(t)$ adopted in this study is a modified form of the power law [25] which assimilate the plasma discharge reactance as a semi conductor dipole.

$$I(t) = I_s \left(\exp\left(\frac{V_g}{n}\right) - 1 \right) \quad (1)$$

$$V_g = V_m \sin(2\pi ft + m\alpha) \quad (2)$$

Where, I_s the current amplitude of saturation current, V_g is the voltage across the plasma reactance -as in (2)- also known as gap voltage, n is a scale factor, V_m the amplitude of the gap voltage, f the frequency of the gap voltage (which is equal to the applied voltage frequency), α represents the phase of the gap voltage, and m it is a correction value that accounts for the memory effect in the second cycle of the applied voltage. This memory effect arises from residual charges left from the preceding half period [15], ($m=1$ for the first cycle, and $2 < m < 2.55$ for the second cycle).

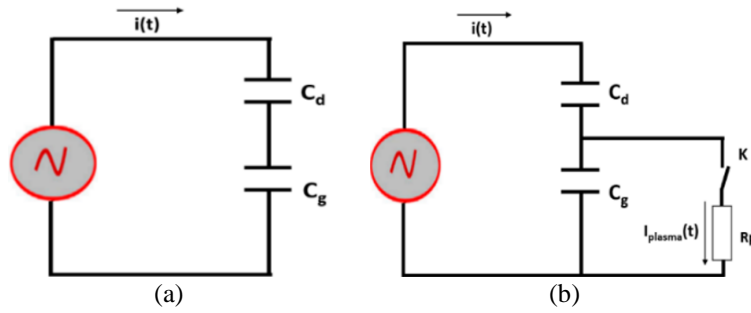


Figure 4. Electrical model for DBD (a) pre-discharge state and (b) discharge phase

To extract the parameters of the proposed model, an initial regression was conducted using the experimental discharge data fitted to the exponential proposed model $I(t)$ as outlined in equation (1). For this regression, only half of the period of the Homogeneous current waveform was utilized. This decision stems from the assumption that the discharge current waveform exhibits symmetry relative to the half-period of the alternative applied voltage. Figure 5 illustrates the overall regression process, an example of the regression fitting is illustrated in Figure 5(a) [19], and the resulting parameters extracted from this model are presented in Table 3.

4.1.1. Gaussian model and parameters extraction

The exponential model exhibits resemblance to a Gaussian wave, as depicted in (3). However, its parameters do not inherently reflect the defining traits of a Gaussian wave, such as center or width. Therefore, a secondary regression to the exponential model was conducted. This regression mapped the parameters of the exponential model, namely I_s , V_m , n , and α , to the Gaussian parameters A , μ , and σ , as illustrated in Figure 5(b). Table 3 presents their corresponding Gaussian parameters, wherein ϕ serves as the correction parameter to account for the memory effect.

$$G(\mu, \sigma) = A \exp \left(-\left(\frac{x-\mu}{\sigma} \right)^2 \right) \quad (3)$$

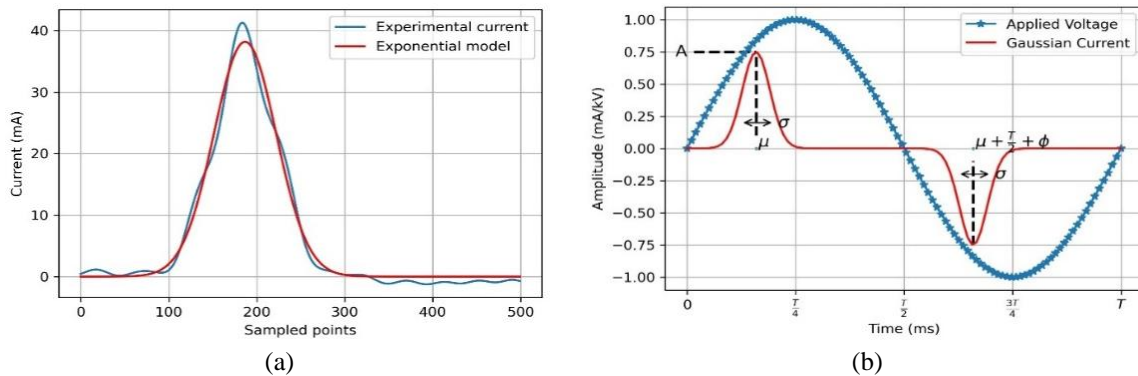


Figure 5. Exponential and Gaussian regressions (a) regression of the proposed exponential model to the experimental current discharge and (b) characteristics of the Gaussian current wave

Table 3. Example of corresponding exponential and Gaussian model parameters

Author	Up (KV)	F (kHz)	d (mm)	V _{bd}	E _d	I _s	V _m	n	α	m	A	μ	σ	ϕ
Garamoon [16]	3	0.05	1.1	3	9	0.38	263.84	126	0.09	2.5	5.63	17.97	11.10	0.86

4.1.2. Gaussian model evaluation

The evaluation of Gaussian regression involved two key metrics. Firstly, the average mean absolute error (AMAE) was computed as the mean absolute difference between the experimental signal currents and their corresponding Gaussian regressed waves. Secondly, the average mean squared error

(AMSE) was calculated as the mean of squared differences between the experimental signal currents and their corresponding Gaussian regressed waves. Figure 6 shows the calculated values of these metrics. Notably, mae_i and mse_i denote the mean absolute error and mean squared error, respectively, between the i -th experimental current wave and its corresponding Gaussian model wave. Specifically, the AMAE was found to be 0.38, while the AMSE was determined to be 0.44.

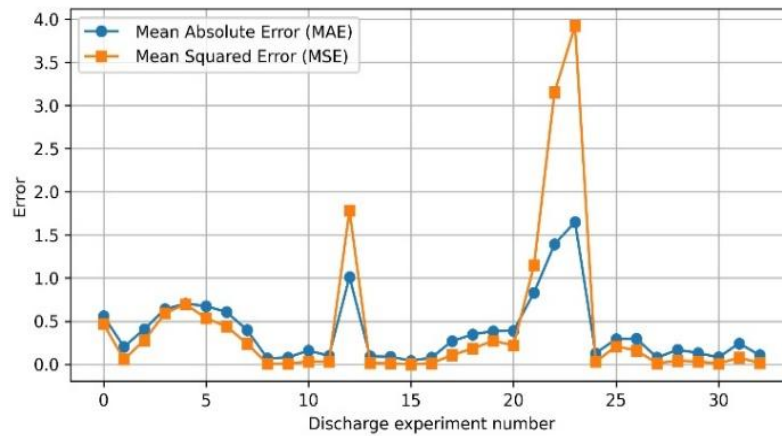


Figure 6. Values of mean absolute and squared errors between the experimental currents and their Gaussian regression

4.2. Random forest regression

In random forest regression, predictions are derived through the averaging of outputs from multiple decision trees, which helps mitigate individual tree biases and enhance overall predictive accuracy. The feature vector is $X_r = [U_p, F, d, V_{bd}, \epsilon_d]$, and the target value is $y_r = [A, \mu, \sigma, \phi]$. Hyperparameters selected for the RandomForestRegressor algorithm consist of the number of trees ($n_estimators = 45$), with the mean squared error ('mse') criterion employed for optimization. Figure 7 provides an overview of the process for extracting parameters from the discharge data. Initially, we derive the parameters of the exponential model, followed by the extraction of Gaussian parameters. These extracted parameters serve as target values for the random forest regression.

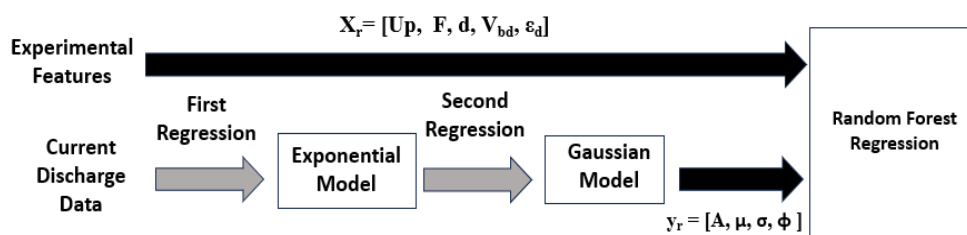


Figure 7. Overview of parameter extraction and schematic structure of the random forest model

4.3. Regression results and evaluation

Figure 8 depicts an example of the random forest regression results by presenting the predicted discharge current waveform with its corresponding experimental discharge current waveform from the test data [16]. The close alignment between the predicted and experimental curves demonstrates the effectiveness of the trained model in capturing the underlying current characteristics. This comparison serves to validate the robustness and predictive capability of the random forest approach for modeling discharge phenomena.

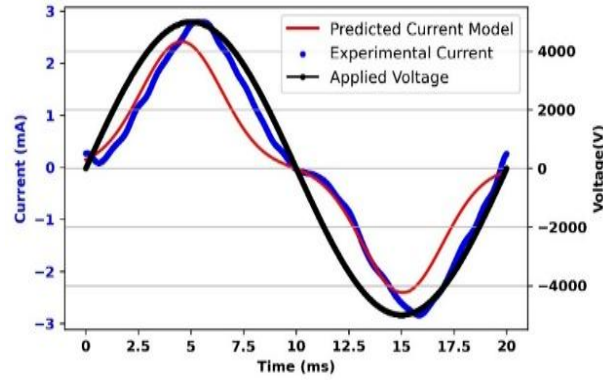


Figure 8. Experimental discharge current waveform and the predicted model current waveform

In evaluating the results of the predicted currents waveforms against the experimental counterparts, the Pearson correlation coefficient was employed to measure the linear relationship between the experimental discharge currents and their associated predicted currents for the test data. Table 4 presents the Pearson correlation coefficient (PCC) for the test data.

Table 4. Correlation coefficient between the predicted and experimental discharge currents

Reference	PCC
Garamoon_1 [16]	0.966
Garamoon_2 [16]	0.969
Osawa [8]	0.965
Ran [11]	0.912
Brandenburg [9]	0.746
Tyata [7]	0.786
Bedoui [18]	0.896

The random forest regression results demonstrate promising correlations between predicted and experimental discharge current waveforms across various reference studies, albeit with some variations. While high Pearson correlation coefficients (PCC) exceeding 0.9 in several cases indicate substantial predictive capability, inconsistencies suggest areas for further improvement. Future enhancements may involve expanding the dataset to include additional discharge experiments and exploring a wider range of features.

5. DISCUSSION

This study demonstrates that machine learning techniques, specifically random forest classification and regression, effectively classify Homogeneous and Filamentary discharge modes in DBD systems and predict Homogeneous discharge currents. Achieving 80% classification accuracy, the model performed strongly using features like applied voltage, gas gap, and dielectric material. The high correlation between predicted and experimental waveforms in regression further supports its ability to predict Homogeneous current waveforms. These results highlight the potential of ML-driven approaches in modelling DBD systems, which traditionally rely on complex physical models. The confusion matrix offers valuable insights into the model's performance and areas for improvement.

Compared to previous studies, this work underscores the advantages of machine learning in plasma system modelling. Unlike research relying heavily on numerical simulations, this study uses data-driven methods, offering greater flexibility and efficiency in addressing nonlinear relationships between features and discharge behaviours. However, misclassifications, particularly false positives where Filamentary discharges were predicted as Homogeneous, remain a limitation. This could stem from feature overlap or insufficient data to fully capture the differences between modes.

The study's primary aim was to explore machine learning applications in classifying discharge modes and predicting discharge currents in DBD systems. It bridges the gap between physical modelling and data-driven approaches, providing insights into non-thermal plasma systems. However, questions remain, such as whether a more diverse dataset could improve performance. Future research should focus on refining feature selection, expanding datasets, and enhancing model sensitivity to reduce misclassifications and improve predictive accuracy.

6. CONCLUSION

In this study, we presented a comprehensive approach to modelling discharge currents in DBD systems using machine learning techniques, specifically random forest classification and regression algorithms. We successfully classified Homogeneous and Filamentary discharge modes and predicted Homogeneous discharge currents with high accuracy in classification and strong correlations between predicted and experimental waveforms in regression. These findings contribute valuable insights to cold plasma research, showing that ML methods can enhance our ability to model and predict DBD behaviours, which have traditionally relied on physical models. The classification model also serves as a valuable tool for understanding the impact of experimental features on discharge modes. However, discrepancies in classification and regression performance suggest the need for further investigation into feature selection, model refinement, and dataset expansion to improve accuracy and robustness. This can lead to better control of plasma processes in industrial, medical, and environmental applications. Overall, our findings highlight the potential of data-driven modelling to advance our understanding of DBD systems and enhance predictive capabilities, with future research focusing on refining models and methodologies for even greater precision.

FUNDING INFORMATION

No funding involved.

AUTHOR CONTRIBUTIONS STATEMENT

Name of Author	C	M	So	Va	Fo	I	R	D	O	E	Vi	Su	P	Fu
Laiadi Abdelhamid	✓	✓	✓		✓	✓		✓	✓	✓	✓			
Chentouf Abdellah	✓	✓		✓		✓		✓	✓	✓	✓	✓		✓
Ezziyani Mustapha	✓		✓	✓			✓					✓	✓	

C : **C**onceptualization

M : **M**ethodology

So : **S**oftware

Va : **V**alidation

Fo : **F**ormal analysis

I : **I**nvestigation

R : **R**esources

D : **D**ata Curation

O : Writing - **O**riginal Draft

E : Writing - Review & **E**ding

Vi : **V**isualization

Su : **S**upervision

P : **P**roject administration

Fu : **F**unding acquisition

CONFLICT OF INTEREST STATEMENT

Authors state no conflict of interest.

DATA AVAILABILITY

Derived data supporting the findings of this study are available from the corresponding author (L. Abdelhamid) on request.




REFERENCES

- [1] R. Brandenburg, K. H. Becker and K.-D. Weltmann, "Barrier discharges in science and technology since 2003: A tribute and update," *Plasma Chemistry and Plasma Processing*, Aug. 2023, doi: 10.1007/s11090-023-10364-5.
- [2] A. Pamreddy *et al.*, "Plasma cleaning and activation of silicon surface in dielectric coplanar surface barrier discharge," *Surface and Coatings Technology*, vol. 236, pp. 326–331, Dec. 2013, doi: 10.1016/j.surfcoat.2013.10.008.
- [3] S. U. Kalghatgi, G. Fridman, A. Fridman, G. Friedman and A. M. Clyne, "Non-thermal dielectric barrier discharge plasma treatment of endothelial cells," *2008 30th Annual International Conference of the IEEE Engineering in Medicine and Biology Society, Vancouver, BC, Canada*, vol. 2008, pp. 3578–3581, 2008, doi: 10.1109/IEMBS.2008.4649979.
- [4] D. Mei and X. Tu, "Conversion of CO₂ in a cylindrical dielectric barrier discharge reactor: Effects of plasma processing parameters and reactor design," *Journal of CO₂ Utilization*, vol. 19, pp. 68–78, May 2017, doi: 10.1016/j.jcou.2017.02.015.
- [5] H. Luo, Z. Liang, B. Lv, X. Wang, Z. Guan and L. Wang, "Observation of the transition from a Townsend discharge to a glow discharge in helium at atmospheric pressure," *Applied Physics. Letter*, vol. 91, no. 22, p. 221504, Nov. 2007, doi: 10.1063/1.2819073.
- [6] F. Massines, N. Gherardi, N. Naudé and P. Ségur, "Glow and Townsend dielectric barrier discharge in various atmosphere," *Plasma Physics and Controlled Fusion*, vol. 47, no. 12B, p. B577, Nov. 2005, doi: 10.1088/0741-3335/47/12B/S42.
- [7] R. Shrestha, R. B. Tyata and D. P. Subedi, "Effect of applied voltage in electron density of homogeneous dielectric barrier discharge at atmospheric pressure," *Himalaya Physics*, vol. 4, pp. 10–13, Dec. 2013, doi: 10.3126/hj.v4i0.9418.
- [8] N. Osawa and Y. Yoshioka, "Generation of low-frequency homogeneous dielectric barrier discharge at atmospheric pressure," *IEEE Transactions on Plasma Science*, vol. 40, no. 1, pp. 2–8, Jan. 2012, doi: 10.1109/TPS.2011.2172634.
- [9] R. Brandenburg, Z. Navrátil, J. Jánský, P. St'ahel, D. Trunc and H.-E. Wagner, "The transition between different modes of barrier discharges at atmospheric pressure," *Journal of Physics D: Applied Physics*, vol. 42, no. 8, p. 085208, Apr. 2009, doi: 10.1088/0022-3727/42/8/085208.




- [10] F. Massines, N. Gherardi, N. Naudé and P. Ségur, "Recent advances in the understanding of homogeneous dielectric barrier discharges," *Eur. Phys. J. - Appl. Phys.*, vol. 47, no. 2, p. 22805, Aug. 2009, doi: 10.1051/epjap/2009064.
- [11] J. Ran, C. Li, D. Ma, H. Luo, and X. Li, "Homogeneous dielectric barrier discharges in atmospheric air and its influencing factor," *Physics Plasmas*, vol. 25, p. 033511, Mar. 2018, doi: 10.1063/1.5019989.
- [12] R. Anirudh *et al.*, "2022 review of data-driven plasma science," *IEEE Transactions on Plasma Science*, vol. 51, no. 7, pp. 1750–1838, Jul. 2023, doi: 10.1109/TPS.2023.3268170.
- [13] T. Guo, X. Liu, S. Hao, X. Gu and X. He, "Prediction of equivalent electrical parameters of dielectric barrier discharge load using a neural network," *Plasma Science and Technology*, vol. 17, no. 3, p. 196, Mar. 2015, doi: 10.1088/1009-0630/17/3/05.
- [14] J. Trieschmann, L. Vialletto and T. Gergs, "Machine learning for advancing low-temperature plasma modeling and simulation," *arXiv*, Jun. 30, 2023, doi: 10.48550/arXiv.2307.00131.
- [15] S. Liu and M. Neiger, "Electrical modelling of homogeneous dielectric barrier discharges under an arbitrary excitation voltage," *Journal of Physics D: Applied Physics*, vol. 36, no. 24, p. 3144, Nov. 2003, doi: 10.1088/0022-3727/36/24/009.
- [16] A. A. Garamoon and D. M. El-zeer, "Atmospheric pressure glow discharge plasma in air at frequency 50 Hz," *Plasma Sources Science and Technology*, vol. 18, no. 4, p. 045006, Nov. 2009, doi: 10.1088/0963-0252/18/4/045006.
- [17] S. Bhosle *et al.*, "Electrical modeling of an homogeneous dielectric barrier discharge (DBD)," in *Fourtieth IAS Annual Meeting. Conference Record of the 2005 Industry Applications Conference, 2005.*, Oct. 2005, pp. 2315-2319 Vol. 4, doi: 10.1109/IAS.2005.1518783.
- [18] M. Bedoui, A. W. Belarbi, and S. Habibes, "Macroscopic modeling of the glow dielectric barrier discharge (GDBD) in helium," *European Journal of Electrical Engineering*, vol. 20, no. 1, pp. 89–103, Feb. 2018, doi: 10.3166/ejee.20.89-103.
- [19] L. Mangolini, C. Anderson, J. Heberlein, and U. Kortshagen, "Effects of current limitation through the dielectric in atmospheric pressure glows in helium," *Journal of Physics D: Applied Physics*, vol. 37, no. 7, p. 1021, Mar. 2004, doi: 10.1088/0022-3727/37/7/012.
- [20] D. M. El-Zeer, A. Samir, F. Elakshar, and A. A. Garamoon, "Decaying of nitrogen second positive system by addition of H₂ gas in air DB discharge," *Journal of Modern Physics*, vol. 4, no. 2, Art. no. 2, Feb. 2013, doi: 10.4236/jmp.2013.42022.
- [21] D. Trunec, A. Brablec and J. Buchta, "Atmospheric pressure glow discharge in neon," *Journal of Physics D: Applied Physics*, vol. 34, no. 11, p. 1697, Jun. 2001, doi: 10.1088/0022-3727/34/11/322.
- [22] E. Alpaydin, *Introduction to Machine Learning*. MIT Press, 2010.
- [23] Z.-H. Zhou, *Ensemble Methods: Foundations and Algorithms*. CRC Press, 2012.
- [24] A. Saridj and A. W. Belarbi, "Numerical modeling of a DBD in glow mode at atmospheric pressure," *Journal of Theoretical and Applied Physics*, vol. 13, no. 3, pp. 179–190, Sep. 2019, doi: 10.1007/s40094-019-00340-w.
- [25] J. A. López-Fernandez *et al.*, "Electrical model of dielectric barrier discharge homogenous and filamentary modes," *Journal of Physics: Conference Series*, vol. 792, p. 012067, Jan. 2017, doi: 10.1088/1742-6596/792/1/012067.

BIOGRAPHIES OF AUTHORS






Laiadi Abdelhamid    He is a Ph.D. student at the Faculty of Science and Technologies in Tangier. He works on the subject of electrical modelling of cold plasma and the dielectric barrier discharge (DBD). He obtained his engineering degree in electronics systems and automation in 2015 from the National School of Applied Sciences of Tangier, Abdelmalek Essaadi University, Morocco. He can be contacted at email: a.laiadi@uae.ac.ma.



Chentouf Abdellah    He is an associate professor at Faculty of Sciences and Technologies of Tangier, Abdelmalek Essaadi University, Morocco, He holds a Ph.D. degree in Energy and Process Engineering from Ecole Central of Nantes, France. His research focuses on the applications of computing and numerical methods for modelling electric and electromagnetic problems. He has developed a package for modelling a RF induction plasma installation and is particularly interested in electrical modelling of cold plasma. He can be contacted at email: achentouf@uae.ac.ma.



Ziani Moustapha    He received the Ph.D. degree in Information System Engineering from Mohammed V University in 1999, Rabat, Morocco. He is a IEEE Member, His research activities focus on advancing data analysis, programming, and machine learning, contributing innovative models for decision support in various fields. He designs effective systems for implementing decision-making processes, empowering organizations to utilize data effectively in practical applications. He is currently a professor of computer Engineering and information System in Faculty of Science and Technologies, Abdelmalek Essaadi University, Morocco. He can be contacted at email: mezziyyani@uae.ac.ma.